Jet quenching and effects of non-Gaussian transverse-momentum broadening on dijet observables

A. van Hameren,[1] K. Kutak,[1] W. Płaczek,[2] M. Rohrmoser,[1] and K. Tywoniuk[3]
[1]*Institute of Nuclear Physics, Polish Academy of Sciences, ulica Radzikowskiego 152, 31-342 Kraków, Poland*
[2]*Institute of Applied Computer Science, Jagiellonian University, ulica Łojasiewicza 11, 30-348 Kraków, Poland*
[3]*Department of Physics and Technology, University of Bergen, 5007 Bergen, Norway*

(Received 19 February 2020; accepted 25 September 2020; published 21 October 2020)

We study, at a qualitative level, production of jet pairs in ultrarelativistic nuclear collisions. We propose a new framework for combining k_T factorization and a formalism for in-medium propagation of jet particles that takes into account stochastic transverse forces as well as medium-induced radiation. This approach allows to address dijet observables accounting for exact kinematics of the initial state. Using our framework, we provide a description of R_{AA} data and study azimuthal decorrelations of the produced dijets. In particular, we find that the resulting dijet observables feature behavior deviating from that of jet pairs which undergo transverse-momentum broadening following the Gaussian distribution. We interpret this behavior as a consequence of dynamics encoded in the Blaizot–Dominguez–Mehtar-Tani–Iancu equation.

DOI: 10.1103/PhysRevC.102.044910

I. INTRODUCTION

A prominent feature of high-energy hadronic collisions is the abundant jet production which is a manifestation of the underlying quantum chromodynamics (QCD). Jets are loosely defined as collimated sprays of particles that act as proxies for the properties of highly virtual partons, quarks and gluons, that participate in the hard scattering. Events where two jets approximately balance their momenta give an additional handle on probing how initial-state processes and their associated parton distribution functions affect the properties of the final-state jets. It is important to point out that such vacuum effects lead to an appreciable azimuthal decorrelation as well as an imbalance of the transverse momentum of the leading and subleading, recoiling, jets.

Jet production in ultrarelativistic nucleus-nucleus collisions has a prominent role in probing the properties of the hot and dense nuclear matter formed in these events [1–3]. This leads to the suppression, or quenching, of high-p_T hadron and inclusive jet spectra observed both at $\sqrt{s_{NN}} = 200$ GeV collisions at RHIC and $\sqrt{s_{NN}} = 5$ TeV collisions at LHC [4,5] (for a review see Ref. [6]). It was early established experimentally that the modifications arose due to final-state interactions. This led to the theoretical development by Baier, Dokshitzer, Mueller, Peigne, Schiff, and Zakharov for the in-medium stimulated (bremsstrahlung) emissions that typically are referred to as the BDMPS-Z formalism [7–10].[1] Such emissions are responsible for transporting energy rapidly away from the jet axis to large angles [12,13]. For high-p_T jets, the total energy loss depends on the fragmentation properties of the jet [14,15] (for the Monte Carlo implementation of these results see Ref. [16]).

In the BDMPS-Z formalism, the medium affects the jet propagation and radiation via transverse momentum exchanges. Typical interactions are described by a diffusion constant $\hat{q}$. In a hot quark-gluon plasma (QGP) it is sensitive to its collective energy density. However, transverse momentum exchange between the jet and the medium is also expected. These are manifestations of the quasiparticles of the hot and dense matter and affect both the spectrum of radiated gluons [17–23] as well as the distribution of particles in transverse momentum space [24,25]. An important question is whether jet observables are sensitive to such interactions, especially those that are sensitive to recoils. For example, the final-state interactions would lead to the gradual decorrelation of jets that originally were created from a vacuum $2 \to 2$ matrix element [26] (see also Refs. [27–29]). In addition, one needs to account for the initial state, i.e., the evolution of the system that leads to hard scattering. It is therefore pertinent to further investigate how the details of the initial state affect the properties of the final state, particularly how the transverse-momentum dependence of the partons initiating the hard collision affect the azimuthal-angle decorrelations of the final-state jets, or the dependence of R_{AA} on the final-state transverse momentum. In approaches that account also for jet quenching, the early stage of heavy-ion (HI) collisions is usually described by the collinear factorization where parton densities obey the

[1]For an equivalent treatment within the thermal field theory see Ref. [11].

Dokshitzer-Gribow-Lipatow-Altarelli-Parisi (DGLAP) evolution equation and the initial-state partons are on mass shell. Consequently, the final-state partons are essentially produced back to back. To account for a nonvanishing transverse-momentum imbalance of the final-state partons, one often uses, on top of medium effects, initial-state parton showers via application of Monte Carlo generators (see, e.g., Refs. [30–34]).

In this paper we propose an approach based on the combination of k_T factorization [35], accounting for the longitudinal and transverse-momentum dependence of matrix elements and parton densities of the initial-state partons,[2] with the evolution in terms of the rate equation based on the final-state jet-plasma interaction. Such an approach allows already at the lowest order, and without application of the initial-state shower (at least up to moderate values of transverse momenta), for a detailed study of the influence of kinematics of the initial state on the properties of the final-state system. We limit ourselves to study observables produced in the mid-forward-rapidity region and, for now, do not account for the initial-state saturation effects [39–41]. Our focus here is to see to what extent the non-Gaussian spectrum of minijets as obtained in Ref. [42] is visible in the final-state observables. The study is rather of a theoretical nature since we only account for gluonic jets. The equations for quarks have not been formulated yet. However, we believe that in the appropriate rapidity range, i.e., the mid-forward region, the observables we are studying are mostly sensitive to gluons but still not to the extent to account for saturation effects [39–41,43]. In order to describe the propagation of partons produced in hard collisions inside a hot quark-gluon plasma, we have applied the recently developed Monte Carlo generator MINCAS [42] that solves the rate equation describing the rescattering and radiation of a hard parton in a dense QCD medium [44] (for a similar approach see Refs. [18,19]).

The paper is organized as follows. In Sec. II we present the theoretical framework of our study. In Sec. III numerical results of our Monte Carlo simulations are presented and discussed. Section concludes this work. Finally, in the Appendix we briefly describe the algorithm used in the numerical simulations.

II. THEORETICAL FRAMEWORK

We factorize the production of a pair of gluon jets in nuclear collisions into the production of a pair of gluons and their subsequent in-medium evolution into gluon jets. The first step is described as the production of two gluons G_1 and G_2 via the hard collision of two gluons G_A and G_B which stem from two nuclei N_A and N_B. We propose to describe this part of the process using the k_T factorization [35,45]. The advantage of this approach is that it allows us to have access to the full phase space already at the leading order (LO) accuracy. The second step is given by the processes of scattering and medium-induced radiation that lead to the fragmentation of G_1 (G_2) into a jet j_1 (j_2). Thus, the total process can be summarized as

$$N_A + N_B \to G_A + G_B + X \to G_1 + G_2 + X \to j_1 + j_2 + X, \tag{1}$$

where X is the production of additional particles which are not used in our descriptions of (di)jet observables. The entire process is depicted schematically in Fig. 1. This section proceeds by first detailing the hard process $N_1 + N_2 \to G_1 + G_2 + X$, then the in-medium propagation $G_i \to j_i$ ($i = 1, 2$), followed by a short description of the modeling of the medium.

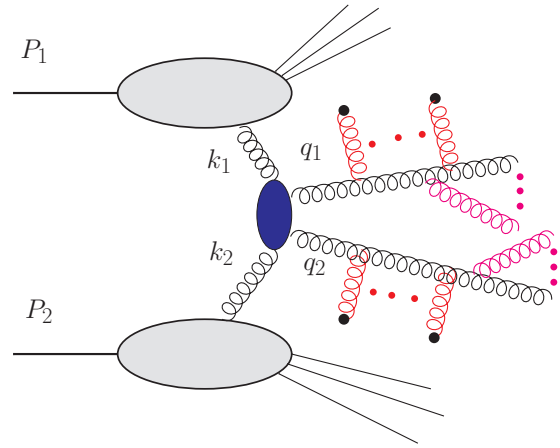

FIG. 1. Gluon-jet production via two scattering gluons in hard nuclear collisions: colliding nuclei (horizontal ellipse) with the momenta P_1 and P_2 yield incoming gluons (with the momenta k_1 and k_2) which interact in a hard-scattering process (vertical ellipse) and yield two gluons (with the momenta q_1 and q_2), which are subject to in-medium scattering (gluon interaction with •), while simultaneously fragmenting into jets denoted in purple.

Jet production at mid-rapidity in proton-proton and heavy-ion collisions is typically computed within collinear factorization. In contrast to most of the existing literature on jets, with the exception of Ref. [26], in this work we consider (relatively) forward jet production within high-energy, or k_T, factorization. This allows to introduce transverse-momentum-dependent (also called unintegrated) parton distributions that resum effects of initial-state showering and the elementary partonic cross section between off-shell partons.

In this approach, the hard coefficient functions are calculated with spacelike initial-state partons. The gauge invariance is guaranteed by adding the so-called induced terms [46,47], which equivalently can be viewed as embedding an off-shell amplitude in an on-shell one of higher order and taking the eikonal limit to decouple auxiliary on-shell lines while preserving terms which guarantee the gauge invariance [48,49].

This factorization is therefore well suited to separate contributions to dijet momentum imbalance and angular decorrelation from the initial state and from final-state radiation and interactions. This is the main motivation for our current exploratory study. We would like to mention that this type of factorization allows to be consistently augmented with a realistic parton shower [37].

[2]For recent phenomenological applications see Refs. [36–38] and references therein.

A. k_T factorization of hard processes

In the k_T factorization the initial-state process reads

$$N_A(P_1) + N_B(P_2) \to G_A(k_1) + G_B(k_2) + X \to G_1(q_1) + G_2(q_2) + X, \tag{2}$$

where the momenta k_1 and k_2 have components transverse to that of the incoming nuclei, an essential property for the description of the dijet observables presented below:

$$k_1 = x_1 P_1 + k_{1T}, \quad k_2 = x_2 P_2 + k_{2T}. \tag{3}$$

The momentum fractions x_i and transverse momenta k_{iT} follow the transverse-momentum distributions for gluons in both of the colliding nuclei given at a certain factorization scale μ_F.

Thus, the k_T-factorization formula for the parton-level differential cross section σ_{pp} at the tree level for the gg pair production reads

$$\frac{d\sigma_{pp}}{dy_1 dy_2 d^2q_{1T} d^2q_{2T}} = \int \frac{d^2k_{1T}}{\pi}\frac{d^2k_{2T}}{\pi}\frac{1}{16\pi^2(x_1x_2s)^2}\overline{\left|\mathcal{M}^{\text{off-shell}}_{g^*g^*\to gg}\right|^2} \times \delta^2(\vec{k}_{1T} + \vec{k}_{2T} - \vec{q}_{1T} - \vec{q}_{2T})\,\mathcal{F}_g\big(x_1, k_{1T}^2, \mu_F^2\big)\mathcal{F}_g\big(x_2, k_{2T}^2, \mu_F^2\big), \tag{4}$$

where $\mathcal{M}^{\text{off-shell}}_{g^*g^*\to g\bar{g}}$ is the off-shell matrix element for the hard subprocess and $\mathcal{F}(x_i, k_{iT}^2, \mu_F^2)$ is the unintegrated gluon density (later on called the transverse-momentum-dependent gluon density (TMD)) which, depending on an approximation used, obeys the Balitsky-Fadin-Kuraev-Lipatov [50,51], Catani-Ciafaloni-Fiorani-Marchesini [45], or Balitsky-Kovchegov [52,53] equation or is given by some model, like that of Golec-Biernat and Wusthoff [54] or Kimber, Martin, Ryskin, and Watt [55]. For the purpose of this work where we address rather moderate values of longitudinal momenta fractions x of partons in incoming hadrons, we use the Martin-Ryskin-Watt gluon densities obtained from the parton distribution functions (PDFs) at next to leading order from [56] (CT10NLO) via the application of the Sudakov form factor.[3] The momentum fractions x_i, the rapidities y_i, and the transverse momenta q_{iT} of the outgoing particles are related to one another as

$$x_1 = \frac{q_{1T}}{\sqrt{s}}\exp(y_1) + \frac{q_{2T}}{\sqrt{s}}\exp(y_2), \quad x_2 = \frac{q_{1T}}{\sqrt{s}}\exp(-y_1) + \frac{q_{2T}}{\sqrt{s}}\exp(-y_2).$$

For the numerical calculation of the hard-process cross sections we rely on the KATIE framework [58], which allows for evaluation of matrix elements and cross sections with off-shell initial-state partons [48,49].

B. In-medium evolution

In this section we describe the processes of the jet evolution in the medium,

$$G_i(q_i) \to j_i(p_i), \quad i = 1, 2\,. \tag{5}$$

The momentum of the jet is modified by its interactions with the medium. We have $\boldsymbol{p} = \boldsymbol{l} + \boldsymbol{q}$, where the $\boldsymbol{l}$ is the change of the jet transverse momentum and $p^+ = \tilde{x}q^+$ is the change of its longitudinal momentum due to momentum exchange with the medium and from the medium-induced branchings.[4] To account for quenching, the cross section σ_{pp} for the production of the vacuum jets should be convoluted with the fragmentation function $D(\tilde{x}, \boldsymbol{l}, \tau)$ for the jets in the medium. Thus, for the inclusive production of the individual jets, the cross section $d\sigma_{AA}/d\Omega_p$ for emission of jets into the phase-space element $d\Omega_p = dp_+ d\boldsymbol{p}$ can be proposed:

$$\begin{aligned}\frac{d\sigma_{AA}}{d\Omega_p} &= \int d\Omega_q \int d^2\boldsymbol{l} \int_0^1 \frac{d\tilde{x}}{\tilde{x}}\,\delta(p^+ - \tilde{x}q^+)\delta^{(2)}(\boldsymbol{p} - \boldsymbol{l} - \boldsymbol{q})D(\tilde{x}, \boldsymbol{l}, \tau(q^+))\frac{d\sigma_{pp}}{d\Omega_q} \\ &= \int d^2\boldsymbol{q} \int_0^1 \frac{d\tilde{x}}{\tilde{x}^2} D(\tilde{x}, \boldsymbol{p} - \boldsymbol{q}, \tau(p^+/\tilde{x}))\left.\frac{d\sigma_{pp}}{dq^+ d^2\boldsymbol{q}}\right|_{q^+ = p^+/\tilde{x}},\end{aligned} \tag{6}$$

where $d\Omega_q = dq^+ d^2\boldsymbol{q}$, $\tau(q^+) = \bar{\alpha}\sqrt{\hat{q}/q^+}L$, and

$$D(\tilde{x}, \boldsymbol{l}, \tau) \equiv \tilde{x}\frac{dN}{d\tilde{x}\, d^2\boldsymbol{l}} \tag{7}$$

---

[3] In the current study, to have a clear picture of broadening due to the non-Gaussian effects, we use just proton TMDs both for the proton-proton and nucleus-nucleus (A-A) collisions, but in the future we plan to use nuclear TMDs (nTMD) for the A-A case [57].

[4] Throughout this article, we use the following notation: The index "T" denotes the momentum components transverse to the beam axis of nuclear collisions, while symbols in boldface represent the momentum components transverse to the jet axis of one of the produced jets. The exception to this convention is the broadening of momenta transverse to the jet axis, which we call the "k_T broadening" in order to be in agreement with many papers written on this subject.

is the distribution of gluons with momentum fraction $\tilde{x}$ and transverse momentum $\boldsymbol{l}$ (relative to the jet axis) after passing through a medium with length L^+ (as encoded in the rescaled evolution variable τ). Similarly for the production of dijets, the differential cross section for the emission of two jets into the phase-space elements $d\Omega_{p_1}$ and $d\Omega_{p_2}$ can be written as

$$\begin{aligned}\frac{d\sigma_{AA}}{d\Omega_{p_1}\Omega_{p_2}} &= \int d\Omega_{q_1} d\Omega_{q_2} \int d^2\boldsymbol{l}_1 \int d^2\boldsymbol{l}_2 \int_0^1 \frac{d\tilde{x}_1}{\tilde{x}_1}\,\delta(p_1^+ - \tilde{x}_1 q_1^+) \int_0^1 \frac{d\tilde{x}_2}{\tilde{x}_2}\,\delta(p_2^+ - \tilde{x}_2 q_2^+) \\ &\quad \times \delta^{(2)}(\boldsymbol{p}_1 - \boldsymbol{l}_1 - \boldsymbol{q}_1)\,\delta^{(2)}(\boldsymbol{p}_2 - \boldsymbol{l}_2 - \boldsymbol{q}_2)\,D(\tilde{x}_1, \boldsymbol{l}_1, \tau(q_1^+))D(\tilde{x}_2, \boldsymbol{l}_2, \tau(q_2^+))\frac{d\sigma_{pp}}{d\Omega_{q_1} d\Omega_{q_2}} \\ &= \int d^2\boldsymbol{q}_1 \int d^2\boldsymbol{q}_2 \int_0^1 \frac{d\tilde{x}_1}{\tilde{x}_1^2} \int_0^1 \frac{d\tilde{x}_2}{\tilde{x}_2^2} D(\tilde{x}_1, \boldsymbol{p}_1 - \boldsymbol{q}_1, \tau(p_1^+/\tilde{x}_1))D(\tilde{x}_2, \boldsymbol{p}_2 - \boldsymbol{q}_2, \tau(p_2^+/\tilde{x}_2)) \\ &\quad \times \frac{d\sigma_{pp}}{dq_1^+ dq_2^+ d^2\boldsymbol{q}_1 d^2\boldsymbol{q}_2}\bigg|_{q_1^+ = p_1^+/\tilde{x}_1,\, q_2^+ = p_2^+/\tilde{x}_2}, \end{aligned} \tag{8}$$

where it is assumed implicitly that the fragmentation processes of jet 1 and jet 2 factorize from the hard-scattering process as well as from each other.

The evolution equation for the gluon transverse-momentum-dependent distribution $D(\tilde{x}, \mathbf{l}, t)$ in the dense medium, obtained under the assumption that the momentum transfer in the kernel is small, reads [44]

$$\frac{\partial}{\partial t} D(\tilde{x}, \mathbf{l}, t) = \frac{1}{t^*} \int_0^1 dz\, \mathcal{K}(z) \left[\frac{1}{z^2} \sqrt{\frac{z}{\tilde{x}}}\, D\Big(\frac{\tilde{x}}{z}, \frac{\mathbf{l}}{z}, t\Big)\theta(z - \tilde{x}) - \frac{z}{\sqrt{\tilde{x}}} D(\tilde{x}, \mathbf{l}, t) \right] + \int \frac{d^2\mathbf{q}}{(2\pi)^2} C(\mathbf{q})\, D(\tilde{x}, \mathbf{l} - \mathbf{q}, t), \tag{9}$$

where

$$\mathcal{K}(z) = \frac{[f(z)]^{5/2}}{[z(1-z)]^{3/2}}, \quad f(z) = 1 - z + z^2, \quad 0 \leqslant z \leqslant 1, \tag{10}$$

is the z-kernel function, and

$$\frac{1}{t^*} = \frac{\bar{\alpha}}{\tau_{\mathrm{br}}(E)} = \bar{\alpha}\sqrt{\frac{\hat{q}}{E}}, \quad \bar{\alpha} = \frac{\alpha_s N_c}{\pi}, \tag{11}$$

where t^* is the stopping time, i.e., the time at which the energy of an incoming parton has been radiated off in the form of soft gluons, E is the energy of the incoming parton, z is its longitudinal momentum fraction, $\hat{q}$ is the quenching parameter, α_s is the QCD coupling constant, and N_c is the number of colors. The kernel $\mathcal{K}(z)$ accounts for soft gluon emissions that are the dominant contribution to jet energy loss. However, the collision kernel $C(\mathbf{q})$ is given by

$$C(\mathbf{q}) = w(\mathbf{q}) - \delta(\mathbf{q}) \int d^2\mathbf{q}'\, w(\mathbf{q}') \tag{12}$$

and includes perturbative, i.e., $\sim 1/\boldsymbol{q}^4$, rescattering with the medium. Here we consider a situation where the quark-gluon plasma equilibrates and the transverse-momentum distribution of medium particles assumes the form [59]

$$w(\mathbf{q}) = \frac{16\pi^2 \alpha_s^2 N_c n}{\mathbf{q}^2\big(\mathbf{q}^2 + m_D^2\big)}, \tag{13}$$

where m_D is the Debye mass of the medium quasiparticles. In the following we consider the expression of Eq. (13) inside the collision kernel $C(\boldsymbol{q})$.

The above integral equations can be formally solved by iteration. Denoting $\tau = t/t^*$, we get [42]

$$\begin{aligned} D(\tilde{x}, \mathbf{l}, \tau) = \int_0^1 d\tilde{x}_0 \int d^2\mathbf{l}_0\, D(\tilde{x}_0, \mathbf{l}_0, \tau_0) \Big\{ & e^{-\Psi(\tilde{x}_0)(\tau - \tau_0)} \delta(\tilde{x} - \tilde{x}_0)\, \delta(\mathbf{l} - \mathbf{l}_0) \\ & + \sum_{n=1}^{\infty} \prod_{i=1}^{n} \left[\int_{\tau_{i-1}}^{\tau} d\tau_i \int_0^1 dz_i \int d^2\mathbf{q}_i\, \mathcal{G}(z_i, \mathbf{q}_i)\, e^{-\Psi(\tilde{x}_{i-1})(\tau_i - \tau_{i-1})} \right] e^{-\Psi(\tilde{x}_n)(\tau - \tau_n)}\, \delta(\tilde{x} - \tilde{x}_n)\, \delta(\mathbf{l} - \mathbf{l}_n) \Big\}, \end{aligned} \tag{14}$$

where

$$\Psi(\tilde{x}) = \Phi(\tilde{x}) + W, \tag{15}$$

$$\Phi(\tilde{x}) = \frac{1}{\sqrt{\tilde{x}}} \int_0^{1-\epsilon} dz\, z \mathcal{K}(z), \tag{16}$$

$$W = t^* \int_{|\mathbf{q}| > q_{\min}} d^2\mathbf{q}\, \frac{w(\mathbf{q})}{(2\pi)^2}, \tag{17}$$

$$\mathcal{G}(z,\mathbf{q}) = \sqrt{\frac{z}{\tilde{x}}}\, z\mathcal{K}(z)\,\theta(1-\epsilon-z)\,\delta(\mathbf{q}) + t^*\,\frac{w(\mathbf{q})}{(2\pi)^2}\,\theta(|\mathbf{q}|-q_{\min})\delta(1-z), \tag{18}$$

and

$$\tilde{x}_n = z_n\tilde{x}_{n-1}, \quad \mathbf{l}_n = z_n\mathbf{l}_{n-1} + \mathbf{q}_n, \tag{19}$$

with $\tilde{x}_0$ and $\mathbf{l}_0$ being some initial values of $\tilde{x}$ and $\mathbf{l}$ at the initial evolution time τ_0, given by the distribution $D(\tilde{x}_0, \mathbf{l}_0, \tau_0)$.

Furthermore, after integration of Eq. (9) over the transverse momentum $\mathbf{l}$ one obtains the evolution equation for the gluon energy density [44]:

$$\frac{\partial}{\partial t}D(\tilde{x},t) = \frac{1}{t^*}\int_0^1 dz\,\mathcal{K}(z)\left[\sqrt{\frac{z}{\tilde{x}}}\,D\Big(\frac{\tilde{x}}{z},t\Big)\theta(z-\tilde{x}) - \frac{z}{\sqrt{\tilde{x}}}\,D(\tilde{x},t)\right], \tag{20}$$

where $D(\tilde{x},t) \equiv \int d^2\boldsymbol{l}\, D(\tilde{x},\boldsymbol{l},t)$. The iterative solution of this equation reads [42]

$$\begin{aligned} D(\tilde{x},\tau) = \int_0^1 d\tilde{x}_0\, D(\tilde{x}_0,\tau_0)\Big\{ & e^{-\Phi(\tilde{x}_0)(\tau-\tau_0)}\,\delta(\tilde{x}-\tilde{x}_0) \\ & + \sum_{n=1}^{\infty}\prod_{i=1}^{n}\left[\int_{\tau_{i-1}}^{\tau} d\tau_i \int_0^1 dz_i \sqrt{\frac{z_i}{\tilde{x}_i}}\, z_i\mathcal{K}(z_i)\,\theta(1-\epsilon-z_i)\, e^{-\Phi(\tilde{x}_{i-1})(\tau_i-\tau_{i-1})}\right] e^{-\Phi(\tilde{x}_n)(\tau-\tau_n)}\,\delta(\tilde{x}-\tilde{x}_n)\Big\}. \end{aligned} \tag{21}$$

Both Eqs. (9) and (20) are solved numerically within the MINCAS framework with the use of dedicated Markov chain Monte Carlo (MCMC) algorithms [42]. In this article, we generally evolve the gluon dijets following the k_T-dependent evolution equation (9) and compare the results to the dijet evolution using Eq. (20) combined with the Gaussian k_T broadening, in order to study the effects of the non-Gaussian k_T broadening.

In both cases, the initial condition for the evolution is a single particle, i.e., $D(\tilde{x},\boldsymbol{l},\tau=0) = \delta(1-x)\delta(\boldsymbol{l})$ [or $D(\tilde{x},\tau=0) = \delta(1-x)$]. After the passage through the medium, medium-induced branching and broadening will generate a collection of particles described by the final distribution $D(\tilde{x},\boldsymbol{l},\tau)$. The notion of the leading particle, which dominates the contribution to the inclusive cross sections, Eqs. (6) and (8), can be recovered in the limit $\tilde{x} \approx 1$.

C. Medium model

Numerous approaches already exist that describe the evolution of the QGP medium with time (cf. Refs. [60,61] and references therein). However, rather than a detailed quantitative description of phenomenology, our current study aims at qualitative understanding of the effects of k_T broadening on dijet evolution. For an isolated study of k_T-broadening effects and for simplicity, we assume that the medium exists for some time t_L with the constant temperature T and is absent at later times. Thus, the medium depends only on two free parameters, while the temperature dependencies of the medium properties that are necessary to describe the jet evolution following Eqs. (9) and (20) can be obtained by phenomenological considerations. The JET Collaboration [62] has obtained the temperature dependence of the transport parameter $\hat{q}$ as

$$\hat{q}(T) = c_q T^3. \tag{22}$$

The number of scattering centers can be estimated by assuming a medium consisting of fermions and bosons at the thermal equilibrium, i.e., by assuming the Fermi-Dirac/Bose-Einstein distributions for the densities of quarks, antiquarks, and gluons, n_q, $n_{\bar{q}}$, and n_g, respectively. As can be shown (cf., e.g., Eq. (3.14) in Ref. [63]), the Taylor expansion in T yields the number densities as the cubic power of T at the lowest orders in T, so that one can write

$$n(T) = n_q + n_{\bar{q}} + n_g = c_n T^3. \tag{23}$$

For the Debye mass m_D we assume that $m_D \propto gT$, which is consistent with findings of the hard thermal loop (HTL) approach. In particular, following Ref. [64], we use the relation

$$m_D^2 = \Big(\frac{N_C}{3} + \frac{N_F}{6}\Big)g^2T^2. \tag{24}$$

In our setup, we have not yet included realistic geometry from the Glauber model for nucleus-nucleus collisions or the effect of the expansion of the medium. This would add more fluctuations to both the path-length distributions as well as the temperature profile probed by the jets. Hence, all partons traverse the same length in the medium, $t_L = \text{const}$, and the same temperature profile. However, while a more realistic geometry certainly is needed to precisely extract medium parameters, these effects were found to be of secondary importance to understand dijet acoplanarity in realistic Monte Carlo studies [65], and will therefore be revisited in the future.

III. NUMERICAL RESULTS

A. Jet-quenching and medium parameters

As outlined in Sec. II C, the effective model for the medium and the jet-medium interactions depends on four parameters, which additionally yield three values that are currently used as parameters within MINCAS. These parameters need to be tuned by comparison to experimental data. Of the aforementioned five parameters, c_q is fixed by phenomenological considerations described in Ref. [62]. Also c_n is fixed, as it is the first coefficient in the Taylor-series expansion of

$n(T)$. Thus, there remain only the two free parameters t_L and T. Assuming that a medium of a diameter of the order of 10 fm is created and that most jets are created in the center of the colliding particles and pass the medium with a velocity close to the speed of light (i.e., ultrarelativistic jet particles), we set the parameter t_L to 5 fm/c. The temperature T is then varied in order to reproduce experimental data on the jet quenching.

With regard to the jets, we have made two essential approximations in order to be able to produce qualitative results for the observables:

(1) Only gluon jets have been considered, since currently evolution equations for quarks analogous to Eq. (9) are not known. To minimize possible errors due to the negligence of quark jets, we consider only observables in a mid-forward-rapidity region where gluon jets dominate.
(2) We identify the momentum of the gluon jet with that of its leading particle. To minimize the possible resulting errors, we consider only leading particles with p_T above a certain threshold.

One of the most inclusive widely studied observables is the nuclear modification ratio R_{AA} as a function of p_T,

$$R_{AA}(p_T) = \frac{1}{\langle T_{AA}\rangle}\frac{dN_{AA}/dp_T}{d\sigma_{pp}/dp_T}, \tag{25}$$

where $\langle T_{AA}\rangle$ is the average nuclear overlap function. For the qualitative considerations of this work, nuclear effects of suppression or enhancement other than jet quenching in the medium have been neglected and the nuclear modification factor is thus approximated as

$$R_{AA}(p_T) \approx \frac{d\sigma_{AA}/dp_T}{d\sigma_{pp}/dp_T}, \tag{26}$$

where $d\sigma_{AA}/dp_T$ is normalized to the number of binary collisions of nucleons in the A-A collision.

In Fig. 2 we show the experimental data from ATLAS on R_{AA} for jets in the Pb-Pb collisions at $\sqrt{s_{NN}} = 2.76$ TeV [66] in comparison with the results from jet simulations with our combination of the KATIE and MINCAS Monte Carlo generators. In order to reproduce the data, the value of T is tuned to 250 MeV. The results for R_{AA} relying on the gluon TMDs and the gluon PDFs both exhibit a considerable suppression, corresponding to values of R_{AA} between 0.4 and 0.6, and, in general, show a similar behavior. However, it can be noted that at the same temperature scales, the results based on the gluon PDFs are at high p_T scales slightly more suppressed than that for the case where gluon distributions depend on transverse momentum. As can be seen, with the chosen value of the temperature our Monte Carlo predictions fit well the data points.

With tuning the temperature scales to the experimental results for R_{AA}, we have fixed all model parameters; they are summarized in Table I.

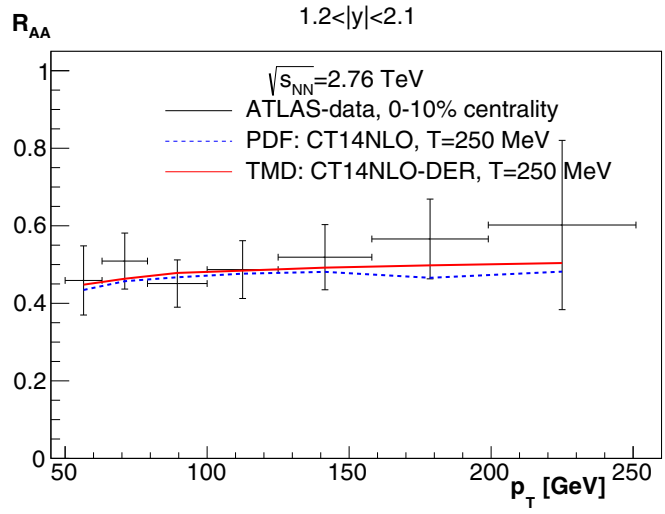

FIG. 2. The nuclear modification factor R_{AA} as a function of the jet transverse momentum p_T for the Pb-Pb collisions at $\sqrt{s_{NN}} = 2.76$ TeV in the mid-forward $1.2 < |y| < 2.1$ region, obtained with the initial-state collinear gluon density (PDFs) and transverse-momentum-dependent (TMD) gluon density as indicated in comparison to the LHC data taken from Ref. [66].

B. Dijet results

As has been already mentioned, the use of the k_T factorization allows to study, already at the LO level, dijet observables in the full phase space, i.e., to have access to regions away from the back-to-back configuration in the transverse plane. In our results, we compare the production of jet pairs in hard collisions without and with further in-medium evolution. The former case, labeled the "vacuum" case, corresponds to, e.g., the dijet production in the proton-proton collisions and was obtained numerically by the use of KATIE alone. Thus, it already contains an asymmetry in the transverse momenta k_T of the jets due to the use of the transverse-momentum-dependent gluon density instead of the gluon PDF. The latter case, labeled the "medium" case, may contain additional k_T-broadening effects of the jet axes due to the jet-medium interactions. We have obtained the results for the medium case by propagating within MINCAS the gluons produced in the hard collisions by KATIE, where the gluon-fragmentation functions follow Eqs. (9) and (20). To further investigate the in-medium k_T broadening we have simulated two different cases:

TABLE I. Parameters for the medium model: the parameters from theoretical and phenomenological considerations (left), the freely adjustable parameters (middle), and the resulting medium parameters used for MINCAS (right).

Fixed		Free		Resulting		
c_q	3.7	t_L	5 fm/c	$\hat{q}$	0.29	GeV^2/fm
c_n	5.228	T	0.25 GeV	n	0.08	GeV^3
				m_D	0.61	GeV

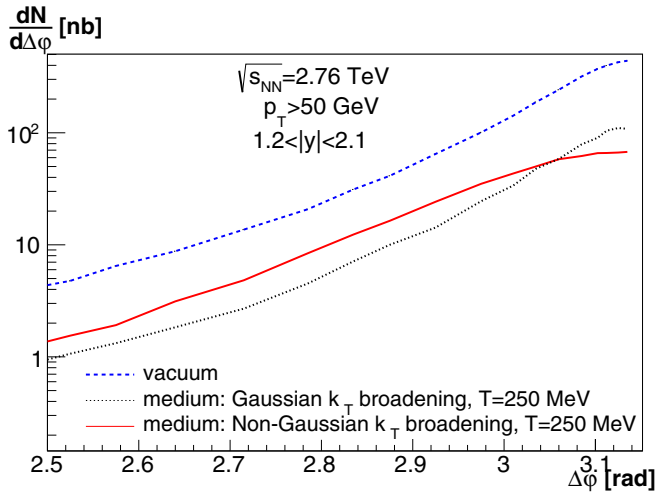

FIG. 3. Azimuthal dijet decorrelations for collisions at $\sqrt{s_{NN}} = 2.76$ TeV between two jets, each with rapidity $1.2 < |y| < 2.1$, as indicated. The results are obtained for the proton-proton collisions (dashed blue line, vacuum) as well as for the Pb-Pb collisions with the k_T broadening as in MINCAS (solid red line, non-Gaussian) and the Gaussian k_T broadening (dotted black line).

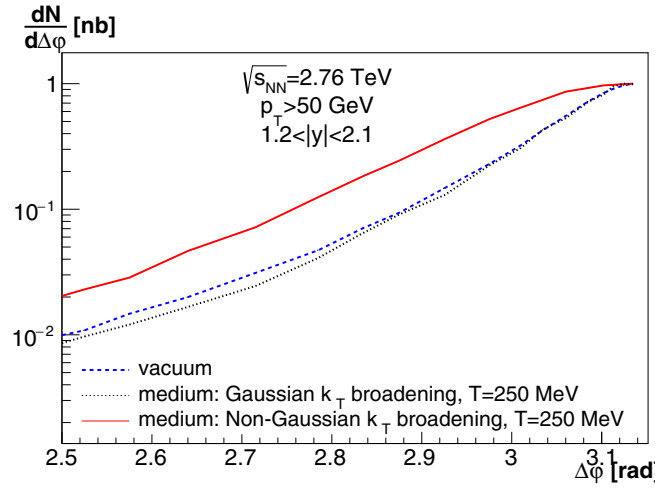

FIG. 4. Same as in Fig. 3, but now normalized to the maximum of the distribution.

(1) In the first case the jet in-medium fragmentation follows Eq. (9). Inside Eq. (9), $C(\boldsymbol{q})$ yields the broadening of momenta transverse to the jet axis. We call this case the "non-Gaussian k_T broadening."

(2) In the second case the loss of jet-momentum components along the jet axis, $\vec{q}_i$ $(i = 1, 2)$, follows Eq. (20). Subsequently, the transverse momentum component $\boldsymbol{l}_i \perp \vec{q}_i$ is selected (for each jet momentum individually) from the Gaussian distribution. As it can be argued that the absolute value of the total transverse-momentum transfer is of the order of $\sqrt{\hat{q}t_L}$, $||\boldsymbol{l}_i||$ is selected from the Gaussian distribution

$$P(||\boldsymbol{l}_i||) = \frac{1}{\sqrt{2\pi\,\hat{q}t_L}}\,\exp\left(-\frac{\boldsymbol{l}_i^2}{2\hat{q}t_L}\right). \qquad (27)$$

The azimuthal angle of the outgoing momenta p_i with regard to q_i is selected randomly from a uniform distribution in the range from zero to 2π. We label the resulting set of jets as "Gaussian k_T broadening."

We study the azimuthal decorrelation $dN/d\Delta\Phi$ given as the number of jet pairs, where $\Delta\Phi$ is the difference in azimuthal angles of the jet axes. The results are shown in Fig. 3 for the dijets where both jets are emitted with transverse momenta p_T above a threshold of 50 GeV and rapidities y in the region $1.2 < |y| < 2.1$. It can be seen that the production of the jet pairs is clearly suppressed in the medium as compared to the production of the jets without the subsequent in-medium propagation. While, compared to the vacuum, the $dN/d\Delta\Phi$ values in the medium are similarly suppressed, whether we assume the Gaussian or non-Gaussian k_T broadening, differences in the behavior of both curves occur, which can be made more visible by normalizing the curves for $dN/d\Delta\Phi$ to the values at their respective maximums $(dN/d\Delta\Phi)_{\max}$. These results are shown in Fig. 4. The case with the non-Gaussian k_T broadening exhibits a clear broadening in $\Delta\Phi$ as compared to the vacuum case, while the case with the Gaussian k_T broadening mostly follows the behavior of the vacuum case.

IV. CONCLUSIONS AND OUTLOOK

We have proposed a factorization formula combining the k_T factorization and medium-jet interactions. Using this formula and its implementation in Monte Carlo generators, we have studied combined effects of transverse momenta of initial-state partons with transverse momenta in the final state generated due to medium-jet interactions. The latter features non-Gaussian behavior due to interplay of radiation and in-medium scattering. The study has been performed using Monte Carlo programs which combine both the hard-scattering process depending on transverse momenta of partons within nucleons and the in-medium evolution for jet particles. To allow for a reasonable jet in-medium evolution, we describe the medium with a simplified effective model that relies merely on two parameters: the time of in-medium jet evolution, t_L, and a constant medium temperature T. This algorithm combines the previously developed frameworks of KATIE [58] and MINCAS [42], and so far is restricted to the production of gluons only.

With the corresponding tuning of T, it has been possible to reproduce the experimental results for the jet nuclear modification factor R_{AA} for the Pb-Pb collisions at $\sqrt{s_{NN}} = 2.76$ TeV. Using the algorithm in this calibration, we have been able to calculate (at a qualitative level, since quarks are missing in our study) the azimuthal dijet decorrelations $dN/d\Delta\Phi$ in Pb-Pb collisions, where we have compared the results for the Gaussian k_T broadening in the medium with that of the non-Gaussian k_T broadening which follows from Eq. (9). Our framework is still too simplistic to really address the full quantitative description of experimental data, since we do not the include vacuumlike emissions in the medium or the parton shower outside the medium [15,16]. However, the effect of the vacuum final-state parton shower on $\Delta\phi$ was studied in Ref. [67] and it was demonstrated that the $\Delta\phi$ distributions obtained using the k_T factorization and PYTHIA

[68] with the final-state parton shower (FSR) agree in shape, while they differ slightly in normalization. When the FSR was neglected the two curves were almost on top of each other. Therefore, we expect that this effect is universal for the vacuum and the medium, and does not influence the comparison of the shapes of both the results. We think that our main result for the azimuthal decorrelations, i.e., the non-Gaussian k_T broadening, is universal and leads to the considerable broadening of the shape of the $dN/d\Delta\phi$ distribution as compared to the Gaussian k_T broadening, as well as to the case of the proton-proton collisions alone.

In the future, we plan to extend our framework to account for quarks which have been neglected in the current study. This will allow us to apply it to phenomenology focused on testing the pattern of jet quenching in jet-jet, jet-hadron [69,70], and jet–electroweak-boson [71,72] final-state systems.

Furthermore, we plan to investigate the broadening due to multiple scatterings in a more forward rapidity region, which is advocated in Ref. [28]. However, this may require accounting for saturation effects [73] which together with the Sudakov effects act to generate considerable broadening in the final-state observables of the p-p and p-Pb collisions [74]. It will be interesting to see the combined effect of the two kinds of broadening.

ACKNOWLEDGMENTS

K.K., A.v.H., and M.R. acknowledge the partial support by the National Centre of Science (Narodowe Centrum Nauki) with Grant No. DEC-2017/27/B/ST2/01985. K.T. is supported by a Starting Grant from Trond Mohn Foundation (Grant No. BFS2018REK01) and the University of Bergen.

APPENDIX: ALGORITHM

Here we outline the algorithm that simulates a hard-scattering process that yields two hard gluons which propagate as leading jet particles through a medium. From a technical point of view, this algorithm merges two Monte Carlo programs: KATIE and MINCAS.

First, KATIE is executed. The center-of-mass energy per nucleon of the hard collision, $\sqrt{s_{NN}}$, needs to be set (2.76 TeV for this work) as well as constraints for the minimum values of the p_T of outgoing particles after the hard collisions. In general, the phase-space boundaries for the hard process, simulated by KATIE, are set larger than those of the finally obtained set of particles (which involves MINCAS as well). Also the factorization scale is set and the sets of TMDs and PDFs are specified. As a scale we use the average of transverse momenta of dijets for this work.

Then, the following steps are repeated for each of the events stored in the output files of KATIE:

(1) From the KATIE output files every event is read in individually. Essential for the algorithm are the outgoing-particle energy E_i and three-momenta $\vec{q}_i$ (with $i = 1, 2$) as well as the weight w of the event.

(2) Polar coordinates for the outgoing-parton three-momenta $\vec{q}_i \equiv (q_{ix}, q_{iy}, q_{iz})$ $(i = 1, 2)$ are calculated as

$$q_i = \sqrt{q_{ix}^2 + q_{iy}^2 + q_{iz}^2}, \tag{A1}$$

$$\theta_i = \arccos q_{iz}/q_i, \tag{A2}$$

$$\phi_i = \arctan q_{iy}/q_{ix}. \tag{A3}$$

The outgoing particles in KATIE are on the mass shell, i.e., $E_i = q_i$.

(3) The following steps are performed for each of the two outgoing particles $i = 1, 2$ individually:

(a) Initialize MINCAS for the particle i. There, as a single parameter from KATIE, the particle energy E_i (before propagation through the medium) is passed in order to calculate t^* via Eq. (11).

(b) A MINCAS event is generated: the function `MINCAS_GenEve` is executed.

(c) `MINCAS_GenEve` yields the fraction $\tilde{x}_i$ with regard to the light-cone energy in the jet frame[5] $q_i^+ = E_i$ as well as the momentum components l_{ix} and l_{iy} in the directions transverse to $\vec{q}_i$. Furthermore, to each jet the Monte Carlo weight ω_i is associated.

(d) The energy E_{p_i} and the momentum component p_{iz} after the in-medium propagation are obtained in the jet frame as

$$E_{p_i} = \tilde{x}_i q_i^+ + \frac{\boldsymbol{l}_i^2}{4\tilde{x}_i q_i^+},$$

$$p_{iz} = \tilde{x}_i q_i^+ - \frac{\boldsymbol{l}_i^2}{4\tilde{x}_i q_i^+}, \tag{A4}$$

while the transverse components of $\vec{p}_i$ are given as $\boldsymbol{l}_i = (l_{ix}, l_{iy})$.

(e) The new momentum $\vec{p}_i$ is rotated back into the laboratory frame:

$$\begin{pmatrix} p_{ix} \\ p_{iy} \\ p_{iz} \end{pmatrix}_{\text{lab}} = \begin{pmatrix} \cos\phi_i & -\sin\phi_i & 0 \\ \sin\phi_i & \cos\phi_i & 0 \\ 0 & 0 & 1 \end{pmatrix} \times \begin{pmatrix} \cos\theta_i & 0 & \sin\theta_i \\ 0 & 1 & 0 \\ -\sin\theta_i & 0 & \cos\theta_i \end{pmatrix} \begin{pmatrix} l_{ix} \\ l_{iy} \\ p_{iz} \end{pmatrix}_{\text{jet}}. \tag{A5}$$

(f) Then, p_{iT} and y_i in the laboratory frame are obtained as

$$p_{iT} = \sqrt{p_{ix}^2 + p_{iy}^2}, \tag{A6}$$

$$y_i = \frac{1}{2} \log \frac{E_{p_i} + p_{iz}}{E_{p_i} - p_{iz}}. \tag{A7}$$

(4) Finally, the event is written as the following three lines into the output file:

$$E_1,\ q_{1x},\ q_{1y},\ q_{1z}, \tag{A8}$$

$$E_2,\ q_{2x},\ q_{2y},\ q_{2z}, \tag{A9}$$

$$p_{1T},\ y_1,\ \phi_1,\ \tilde{x}_1,\ p_{2T},\ y_2,\ \phi_2,\ \tilde{x}_2,\ \omega_1,\ \omega_2,\ w. \tag{A10}$$

[5]For this purpose, we define the jet frame as the one obtained after the rotation of the coordinate system in the laboratory frame, such that $\vec{q}_i$ is parallel to the z axis of the new coordinate system.

[1] D. d'Enterria, Jet quenching, in *Relativistic Heavy Ion Physics, Landolt-Bornstein—Group I Elementary Particles, Nuclei and Atoms Vol. 23* (Springer, Berlin, 2010), p. 471.

[2] Y. Mehtar-Tani, J. G. Milhano, and K. Tywoniuk, Jet physics in heavy-ion collisions, Int. J. Mod. Phys. A **28**, 1340013 (2013).

[3] J.-P. Blaizot and Y. Mehtar-Tani, Jet structure in heavy ion collisions, Int. J. Mod. Phys. E **24**, 1530012 (2015).

[4] G. Aad *et al.* (ATLAS Collaboration), Observation of a Centrality-Dependent Dijet Asymmetry in Lead-Lead Collisions at $\sqrt{s_{NN}} = 2.77$ TeV with the ATLAS Detector at the LHC, Phys. Rev. Lett. **105**, 252303 (2010).

[5] S. Chatrchyan *et al.* (CMS Collaboration), Observation and studies of jet quenching in PbPb collisions at nucleon-nucleon center-of-mass energy = 2.76 TeV, Phys. Rev. C **84**, 024906 (2011).

[6] G.-Y. Qin and X.-N. Wang, Jet quenching in high-energy heavy-ion collisions, Int. J. Mod. Phys. E **24**, 1530014 (2015).

[7] R. Baier, Y. L. Dokshitzer, A. H. Mueller, S. Peigne, and D. Schiff, Radiative energy loss of high-energy quarks and gluons in a finite volume quark-gluon plasma, Nucl. Phys. B **483**, 291 (1997).

[8] R. Baier, Y. L. Dokshitzer, A. H. Mueller, S. Peigne, and D. Schiff, Radiative energy loss and $p_\perp$-broadening of high-energy partons in nuclei, Nucl. Phys. B **484**, 265 (1997).

[9] B. G. Zakharov, Fully quantum treatment of the Landau-Pomeranchuk-Migdal effect in QED and QCD, JETP Lett. **63**, 952 (1996).

[10] B. G. Zakharov, Radiative energy loss of high-energy quarks in finite size nuclear matter and quark-gluon plasma, JETP Lett. **65**, 615 (1997).

[11] P. B. Arnold, G. D. Moore, and L. G. Yaffe, Photon and gluon emission in relativistic plasmas, J. High Energy Phys. 06 (2002) 030.

[12] J.-P. Blaizot, E. Iancu, and Y. Mehtar-Tani, Medium-Induced QCD Cascade: Democratic Branching and Wave Turbulence, Phys. Rev. Lett. **111**, 052001 (2013).

[13] A. Kurkela and U. A. Wiedemann, Picturing perturbative parton cascades in QCD matter, Phys. Lett. B **740**, 172 (2015).

[14] Y. Mehtar-Tani and K. Tywoniuk, Sudakov suppression of jets in QCD media, Phys. Rev. D **98**, 051501 (2018).

[15] P. Caucal, E. Iancu, A. H. Mueller, and G. Soyez, Vacuum-Like Jet Fragmentation in a Dense QCD Medium, Phys. Rev. Lett. **120**, 232001 (2018).

[16] P. Caucal, E. Iancu, and G. Soyez, Deciphering the z_g distribution in ultrarelativistic heavy ion collisions, J. High Energy Phys. 10 (2019) 273.

[17] S. Caron-Huot and C. Gale, Finite-size effects on the radiative energy loss of a fast parton in hot and dense strongly interacting matter, Phys. Rev. C **82**, 064902 (2010).

[18] X. Feal and R. Vazquez, Intensity of gluon bremsstrahlung in a finite plasma, Phys. Rev. D **98**, 074029 (2018).

[19] X. Feal and R. A. Vazquez, Transverse spectrum of bremsstrahlung in finite condensed media, Phys. Rev. D **99**, 016002 (2019).

[20] X. Feal, C. A. Salgado, and R. A. Vazquez, Jet quenching tests of the QCD equation of state, arXiv:1911.01309.

[21] W. Ke, Y. Xu, and S. A. Bass, Modified Boltzmann approach for modeling the splitting vertices induced by the hot QCD medium in the deep Landau-Pomeranchuk-Migdal region, Phys. Rev. C **100**, 064911 (2019).

[22] Y. Mehtar-Tani, Gluon bremsstrahlung in finite media beyond multiple soft scattering approximation, J. High Energy Phys. 07 (2019) 057.

[23] Y. Mehtar-Tani and K. Tywoniuk, Improved opacity expansion for medium-induced parton splitting, J. High Energy Phys. 06 (2020) 187.

[24] F. D'Eramo, H. Liu, and K. Rajagopal, Transverse momentum broadening and the jet quenching parameter, redux, Phys. Rev. D **84**, 065015 (2011).

[25] F. D'Eramo, M. Lekaveckas, H. Liu, and K. Rajagopal, Momentum broadening in weakly coupled quark-gluon plasma (with a view to finding the quasiparticles within liquid quark-gluon plasma), J. High Energy Phys. 05 (2013) 031.

[26] M. Deák, K. Kutak, and K. Tywoniuk, Towards tomography of quark-gluon plasma using double inclusive forward-central jets in Pb-Pb collision, Eur. Phys. J. C **77**, 793 (2017).

[27] A. H. Mueller, B. Wu, B.-W. Xiao, and F. Yuan, Probing transverse momentum broadening in heavy ion collisions, Phys. Lett. B **763**, 208 (2016).

[28] J. Jia, S.-Y. Wei, B.-W. Xiao, and F. Yuan, Medium-induced transverse momentum broadening via forward dijet correlations, Phys. Rev. D **101**, 094008 (2020).

[29] F. Ringer, B.-W. Xiao, and F. Yuan, Can we observe jet P_T-broadening in heavy-ion collisions at the LHC? Phys. Lett. B **808**, 135634 (2020).

[30] C. A. Salgado and U. A. Wiedemann, Calculating quenching weights, Phys. Rev. D **68**, 014008 (2003).

[31] K. Zapp, G. Ingelman, J. Rathsman, J. Stachel, and U. A. Wiedemann, A Monte Carlo model for "jet quenching", Eur. Phys. J. C **60**, 617 (2009).

[32] N. Armesto, L. Cunqueiro, and C. A. Salgado, Q-PYTHIA: A medium-modified implementation of final state radiation, Eur. Phys. J. C **63**, 679 (2009).

[33] B. Schenke, C. Gale, and S. Jeon, MARTINI: An event generator for relativistic heavy-ion collisions, Phys. Rev. C **80**, 054913 (2009).

[34] I. P. Lokhtin, A. V. Belyaev, and A. M. Snigirev, Jet quenching pattern at LHC in PYQUEN model, Eur. Phys. J. C **71**, 1650 (2011).

[35] S. Catani, M. Ciafaloni, and F. Hautmann, High-energy factorization and small-x heavy flavour production, Nucl. Phys. B **366**, 135 (1991).

[36] M. Deak, A. van Hameren, H. Jung, A. Kusina, K. Kutak, and M. Serino, Calculation of the Z+jet cross section including transverse momenta of initial partons, Phys. Rev. D **99**, 094011 (2019).

[37] M. Bury, A. van Hameren, H. Jung, K. Kutak, S. Sapeta, and M. Serino, Calculations with off-shell matrix elements, TMD parton densities and TMD parton showers, Eur. Phys. J. C **78**, 137 (2018).

[38] K. Kutak, R. Maciuła, M. Serino, A. Szczurek, and A. van Hameren, Search for optimal conditions for exploring double-parton scattering in four-jet production: k_t-factorization approach, Phys. Rev. D **94**, 014019 (2016).

[39] L. V. Gribov, E. M. Levin, and M. G. Ryskin, Semihard processes in QCD, Phys. Rep. **100**, 1 (1983).

[40] F. Gelis, E. Iancu, J. Jalilian-Marian, and R. Venugopalan, The color glass condensate, Annu. Rev. Nucl. Part. Sci. **60**, 463 (2010).
[41] Y. V. Kovchegov and E. Levin, *Quantum Chromodynamics at High Energy* (Cambridge University Press, Cambridge, UK, 2012), Vol. 33.
[42] K. Kutak, W. Płaczek, and R. Straka, Solutions of evolution equations for medium-induced QCD cascades, Eur. Phys. J. C **79**, 317 (2019).
[43] A. van Hameren, P. Kotko, K. Kutak, and S. Sapeta, Small-x dynamics in forward-central dijet decorrelations at the LHC, Phys. Lett. B **737**, 335 (2014).
[44] J.-P. Blaizot, L. Fister, and Y. Mehtar-Tani, Angular distribution of medium-induced QCD cascades, Nucl. Phys. A **940**, 67 (2015).
[45] S. Catani, F. Fiorani, and G. Marchesini, QCD coherence in initial state radiation, Phys. Lett. B **234**, 339 (1990).
[46] L. N. Lipatov, Gauge invariant effective action for high-energy processes in QCD, Nucl. Phys. B **452**, 369 (1995).
[47] L. N. Lipatov, Small-x physics in perturbative QCD, Phys. Rep. **286**, 131 (1997).
[48] A. van Hameren, P. Kotko, and K. Kutak, Helicity amplitudes for high-energy scattering, J. High Energy Phys. 01 (2013) 078.
[49] A. van Hameren, P. Kotko, and K. Kutak, Multi-gluon helicity amplitudes with one off-shell leg within high energy factorization, J. High Energy Phys. 12 (2012) 029.
[50] V. S. Fadin, E. A. Kuraev, and L. N. Lipatov, On the Pomeranchuk singularity in asymptotically free theories, Phys. Lett. B **60**, 50 (1975).
[51] I. I. Balitsky and L. N. Lipatov, The Pomeranchuk singularity in quantum chromodynamics, Sov. J. Nucl. Phys. **28**, 822 (1978) [Yad. Fiz. **28**, 1597 (1978)].
[52] I. Balitsky, Operator expansion for high-energy scattering, Nucl. Phys. B **463**, 99 (1996).
[53] Y. V. Kovchegov, Small-xF_2 structure function of a nucleus including multiple Pomeron exchanges, Phys. Rev. D **60**, 034008 (1999).
[54] K. J. Golec-Biernat and M. Wusthoff, Saturation effects in deep inelastic scattering at low Q^2 and its implications on diffraction, Phys. Rev. D **59**, 014017 (1998).
[55] A. D. Martin, M. G. Ryskin, and G. Watt, NLO prescription for unintegrated parton distributions, Eur. Phys. J. C **66**, 163 (2010).
[56] H-L Lai *et al.*, New parton distributions for collider physics, Phys. Rev. D **82**, 074024 (2010).
[57] E. Blanco, A. van Hameren, H. Jung, A. Kusina, and K. Kutak, Z boson production in proton-lead collisions at the LHC accounting for transverse momenta of initial partons, Phys. Rev. D **100**, 054023 (2019).
[58] A. van Hameren, KaTie: For parton-level event generation with k_T-dependent initial states, Comput. Phys. Commun. **224**, 371 (2018).
[59] P. Aurenche, F. Gelis, and H. Zaraket, A simple sum rule for the thermal gluon spectral function and applications, J. High Energy Phys. 05 (2002) 043.
[60] W. Florkowski, *Phenomenology of Ultra-Relativistic Heavy-Ion Collisions* (World Scientific, Singapore, 2010).
[61] A. Jaiswal and V. Roy, Relativistic hydrodynamics in heavy-ion collisions: General aspects and recent developments, Adv. High Energy Phys. **2016**, 9623034 (2016).
[62] K. M. Burke (JET Collaboration) *et al.*, Extracting the jet transport coefficient from jet quenching in high-energy heavy-ion collisions, Phys. Rev. C **90**, 014909 (2014).
[63] K. C. Zapp, A Monte Carlo model for jet evolution with energy loss, Ph.D. thesis, Heidelberg University, 2008.
[64] M. Laine and A. Vuorinen, Quantum mechanics, in *Basics of Thermal Field Theory, Lecture Notes in Physics* Vol. 925 (Springer, Berlin, 2016), p. 1.
[65] J. G. Milhano and K. C. Zapp, Origins of the di-jet asymmetry in heavy ion collisions, Eur. Phys. J. C **76**, 288 (2016).
[66] G. Aad *et al.* (ATLAS Collaboration), Measurements of the Nuclear Modification Factor for Jets in Pb+Pb Collisions at $\sqrt{s_{\rm NN}} = 2.76$ TeV with the ATLAS Detector, Phys. Rev. Lett. **114**, 072302 (2015).
[67] M. Bury, M. Deak, K. Kutak, and S. Sapeta, Single and double inclusive forward jet production at the LHC at $\sqrt{s} = 7$ and 13 TeV, Phys. Lett. B **760**, 594 (2016).
[68] T. Sjöstrand, S. Ask, J. R. Christiansen, R. Corke, N. Desai, P. Ilten, S. Mrenna, S. Prestel, C. O. Rasmussen, and P. Z. Skands, An introduction to PYTHIA 8.2, Comput. Phys. Commun. **191**, 159 (2015).
[69] J. Adam *et al.* (ALICE Collaboration), Measurement of jet quenching with semi-inclusive hadron-jet distributions in central Pb-Pb collisions at $\sqrt{s_{\rm NN}} = 2.76$ TeV, J. High Energy Phys. 09 (2015) 170.
[70] L. Adamczyk (STAR Collaboration) *et al.*, Measurements of jet quenching with semi-inclusive hadron+jet distributions in Au+Au collisions at $\sqrt{s_{NN}} = 200$ GeV, Phys. Rev. C **96**, 024905 (2017).
[71] A. M. Sirunyan *et al.* (CMS Collaboration), Study of Jet Quenching with $Z +$ Jet Correlations in Pb-Pb and pp Collisions at $\sqrt{s_{NN}} = 5.02$ TeV, Phys. Rev. Lett. **119**, 082301 (2017).
[72] ATLAS Collaboration, Measurement of Z-tagged charged-particle yields in 5.02 TeV Pb+Pb and pp collisions with the ATLAS detector (unpublished).
[73] A. van Hameren, P. Kotko, K. Kutak, and S. Sapeta, Broadening and saturation effects in dijet azimuthal correlations in p-p and p-Pb collisions at $\sqrt{s_{NN}} = 5.02$ TeV, Phys. Lett. B **795**, 511 (2019).
[74] M. Aaboud *et al.* (ATLAS Collaboration), Dijet azimuthal correlations and conditional yields in pp and $p +$ Pb collisions at $\sqrt{s_{NN}} = 5.02$ TeV with the ATLAS detector, Phys. Rev. C **100**, 034903 (2019).